forests

Article

Seasonality of Photosynthetic Physiology and Leaf Anatomy in Three Different *Quercus* L. Section *Cyclobalanopsis* Seedlings of *Quercus chungii, Quercus gilva, and Quercus glauca* in the Subtropical Region of South China

Hui-Min Yin [1,2], Mo-Hua Yang [1,2,*], Peng-Le Li [1,2], Xun-Lin Yu [1,2], Huan Xiong [1,2], Qian-Yu Xu [1,2], Feng-Lan Zou [1,2], You Chen [1,2], Wei-Hong Dai [1,2], Yin Jiang [1,2] and Yue-Lin Li [3,*]

[1] College of Forestry, Central South University of Forestry and Technology, Changsha 410004, China
[2] National Long Term Experimental Base of Forestry in Mid-Subtropics of China, Central South University of Forestry and Technology, Changsha 410004, China
[3] Key Laboratory of Vegetation Restoration and Management of Degraded Ecosystems, South China Botanical Garden, Chinese Academy of Sciences, Guangzhou 510650, China
* Correspondence: mohua.yang@csuft.edu.cn (M.-H.Y.); yuelin@scib.ac.cn (Y.-L.L.)

Citation: Yin, H.-M.; Yang, M.-H.; Li, P.-L.; Yu, X.-L.; Xiong, H.; Xu, Q.-Y.; Zou, F.-L.; Chen, Y.; Dai, W.-H.; Jiang, Y.; et al. Seasonality of Photosynthetic Physiology and Leaf Anatomy in Three Different *Quercus* L. Section *Cyclobalanopsis* Seedlings of *Quercus chungii, Quercus gilva, and Quercus glauca* in the Subtropical Region of South China. *Forests* **2022**, *13*, 2067. https://doi.org/10.3390/f13122067

Academic Editors: Eva Pšidová, Srdjan Stojnic and Katarína Střelcová

Received: 25 October 2022
Accepted: 30 November 2022
Published: 4 December 2022

Abstract: The increasing demand for precious timber resources promotes immediate efforts to develop high-valuable hardwood resources in afforestation. However, the lack of valuable tree species seedlings for afforestation and their ecological adaptability must primarily be addressed. To explore a valuable tree species for precious timber resourcing in afforestation, a comparative analysis of the characteristics of photosynthetic physiology and leaf anatomy in three different *Quercus* L. Section *Cyclobalanopsis* seedlings of *Quercus chungii, Quercus gilva*, and *Quercus glauca* was performed during three growth stages (July, September, and November) in South China. The results showed that there are significant differences in photosynthetic physiological characteristic parameters, chlorophyll content, and leaf anatomical structure among the three seedlings in each growth stage ($p < 0.05$). The photosynthetic parameters, i.e., *Pn*, *Gs*, *Tr, WUE* and *Ci* in each tree species all had the same trend of increase from July to September and decrease from September to November, and with a pick point in September during the three stages. The *Pn* in *Q. chungii* was higher than that in the other two species in each stage, and the highest *Pn* with an average value of 8.26 $\mu mol \cdot m^{-2} \cdot s^{-1}$ was obtained in September in *Q. chungii*, which was 13.77% and 20.06% higher than that of in *Q. gilva* and *Q. glauca* at the same time, respectively. Significant differences were also detected in the chlorophyll fluorescence of *Fo*, *Fm*, *Fv*/*Fm*, *Y*, *ETR*, *qP*, and *NPQ* among three seedlings within each growth stage from July to November ($p < 0.05$). The thickness of the mature leaf was decreased in order as *Q. chungii*, *Q. glauca*, and *Q. gilva*. From July to September, more notable changes were observed in *Q. chungii* in September, with a drop of 3.49% in leaf thickness, and a drop of 3.34% and 10.06% in the volume of palisade tissue and sponge tissue, respectively. Consequently, increasing tightness and deducing looseness were observed in *Q. chungii*. The principal component analysis (PCA) on photosynthesis and leaf anatomy showed that *Q. chungii* displayed a stronger photosynthetic physiology with a positive coordination on water, air, light, and heat. These findings facilitate the evaluation of ecological adaptability among the three *Quercus* seedlings and provide compelling evidence for the application of *Q. chungii* for precious timber resources in afforestation.

Keywords: *Quercus chungii*; *Quercus gilva*; *Quercus glauca*; photosynthesis characteristics; leaf anatomy; afforestation

1. Introduction

The shortage of precious timber resources promotes immediate efforts to develop high-value and end-use timber resources in afforestation. However, the lack of suitable precious timber tree species and the evaluation of the ecological adaptability of its seedlings in the installation of afforestation remain to be settled first. The *Quercus* L, commonly known as oaks, is the largest genus of the Fagaceae family, with more than 400 species native to the Northern Hemisphere [1–3]. The *Quercus* is also famous as one of the most majestic trees, prized around the world for its towering elegance and sturdy timber, which places them as first choice for precious timber tree species for afforestation [4]. The three *Quercus* L. Section *Cyclobalanopsis* of *Quercus chungii* (*Cyclobalanopsis chungii* in Flora of China), *Quercus gilva*, and *Quercus glauca* are treated as traditional precious timber resources, due to their outstanding decorative appearance and special technical properties harbored in the straight trunk, wood density, resistance to wear, corrosion, and moisture [5]. The two oaks (*Q. chungii* and *Q. gilva*) are famous for their reddish-brown wood and the other (*Q. glauca*) has beautiful wood patterns in the brown wood. However, *Q. chungii* is a threatened species in the Red List of Oaks 2020 with limited distribution endemic to South China [6], and it has now been listed as a third-class rare and endangered protected plant in Fujian Province [7]. A rare case of thirties year's afforestation of *Q. chungii* has showed a strong ecological adaptability with medium to high growth in the drought and sterile environment, compared to plantation of the Chinese fir (*Cunninghamia lanceolata*) at the same site [8]. *Q. gilva* has been the popular afforestation tree species used for precious timber tree resources in South China over the last decade. Several studies have revealed the physiological characteristics of *Q. gilva* at different seedling stages and forest ages [9–11], its characteristics on growth, and its ecological environment requirements [12]. The *Q. glauca* was an essential tree species for restoration for a long time due to its high resistance to drought, given it is barren tolerance in the karst rocky desertification area [13]. Unlike these two *Cyclobalanopsis* cultivated for some time, *Q. chungii* remains a potentially precious timber tree species for afforestation, with the most outstanding decorative appearance of a reddish-brown wood without distinction from heartwood and sapwood. However, little is known about its ecological adaptability in the installation of afforestation in the field, as accounted for by its poor natural regeneration capability with endemic distribution of a narrow distribution range [7], compared to the other two *Cyclobalanopsis* of *Q. gilva* and *Q. glauca.* The genetic resource investigation on *Q. chungii* showed that *Q. chungii* trees are found scattered in Hunan, Guangdong, Jiangxi, and Fujian province, except for the only one larger protected area in Fujian Minqing Huangchu Forest Nature Reserve (FMHFNR). It would therefore be of interest to know the extent of the ecological adaptability of the threatened *Q. chungii* seedlings, especially compared to the other two oak species in the same habitat, namely within the *Quercus* L. section *Cyclobalanopsis*, such as *Q. gilva* and *Q. glauca*.

The seedling is the key development stage in afforestation, and evaluation of the ecological adaptability of the seedings has played an important role in its successful installation under field conditions. The adaptations to environmental stress are mainly illustrated in the characteristics of photosynthesis and leaf anatomy of a tree species [14,15]. Considerable efforts have been taken to measure the photosynthetic physiological characteristics and anatomical structure of forest tree species seedlings to evaluate their adaptation and potential growth capacity under field conditions. Climate change will lead to a high risk of maladaptation of tree species and the maladaptive plasticity is clearly detrimental to adaptation [16]. Failure of regeneration of *Q. chungii* in the population of FMHFNR would provoke great concern about its maladaptation to local conditions [7]. Higher photosynthetic physiology resulted in higher seedling survival in European yew (*Taxus baccata* L.) and the phenotypic plasticity was also observed in leaf anatomy response to environmental stress [14,17]. It is necessary to explore the differences in photosynthesis and leaf anatomy among the three *Quercus* L. section *Cyclobalanopsis* to illustrate the different potential adaptations of afforestation tree species to the changing global climate warming environment for the selection of precious timber tree species in afforestation.

Plant photosynthesis is a complex biological, physical, and chemical process in which plants convert light energy into chemical energy and carry out organic matter synthesis, which is the prerequisite and basis of all physiological activities of plants, and the level of photosynthetic efficiency reflects not only the efficiency of light energy utilization in plants but also their growth potential and their stress resistance capacity [17,18]. Photosynthetic gas exchange parameters and chlorophyll fluorescence measurements are two commonly used approaches to study plant photosynthesis [19,20]. Differential photosynthetic responses of *Q. gilva* display heterogeneous changes in different habitats [11], and adaptive changes in the anatomical structure of *Q. gilva* leaves are observed under the different water stress [21,22]. Studies on drought stress and chlorophyll fluorescence of *Q. glauca* showed that the seedlings had a strong drought tolerance [23,24]. In particular, studies on the survival of annual *Taxus baccata* L. seedlings showed that those with higher chlorophyll pigment content under optimal light conditions had higher photosynthetic rates and higher seedling survival [17]. A significant divergence was observed between two closely related *Cyclobalanopsis species* (*C.helferiana* and *C. rex*) seedlings in photosynthetic characteristics, accounting for their different adaptation and acclimation to same natural conditions [25]. Comparison of the photosynthetic physiological and anatomical structure characteristics in the natural environment between the protected oak (*Q. chungii*) and the stable oaks (*Q. gilva* and *Q. glauca*) would provide essential reference of empirical evidence of phenotypic plasticity to local conditions for the evaluation of protected *Quercus* L. section *Cyclobalanopsis* seedlings in afforestation.

This study measured the photosynthetic gas exchange parameters, chlorophyll fluorescence parameters, and photosynthetic pigment content of the leaves of the three species seedlings in July, September, and November. Paraffin sections of mature leaves of the seedlings in the three species were made simultaneously to observe the differences in mature leaves' anatomical structure of the seedlings in the three species at different seasons. The specific objectives of this study were to explore the seasonality of photosynthetic physiology and leaf anatomy of seedlings in three precious tree species, to evaluate their ecological adaptability in afforestation, and characterize the differences in photosynthetic physiology and leaf anatomy of seedlings among the three precious tree species under natural environmental conditions. It is our hope to provide a practical understanding of precious timber tree species source exploration to select high light efficiency and high resistance potential tree species for afforestation in South China.

2. Materials and Methods

2.1. Overview of the Study Site and Species

The experimental site was located at the campus of Central South University of Forestry and Technology in Changsha, Hunan Province (28°14′49″ N, 112°99′42″ E). The region is located in Central China, belonging to the subtropical monsoon with abundant rainfall and heat, with an annual average temperature of 16.8–17.2 °C. There is no frost for about 275 days. There are distinct dry and wet seasons in the year, with an annual average rainfall of 1450 mm.

In the genus of *Cyclobalanopsis* (Fagaceae), three evergreen tree species were studied in the present investigation. The distribution range, habitat type, and environmental adaptations of the three species were distinctly different. In October 2020, the seeds of superior tree species of *Q. chungii*, *Q. gilva*, and *Q. glauca* were collected in Guangdong and Hunan provinces which were adopted by standardized sowing and seedling raising. In May 2021, one-year-old seedlings with healthy and consistent growth were selected. They were then placed in pots (25 cm in height and 20 cm in diameter) containing 1 kg of media substrate with shaded rates of 50%. The substrate consisted of acidic red soil, peat (Klasmann, Niedersachsen, Germany), and perlite mixed at a ratio of 3:2:1 ($v/v/v$).

2.2. Experimental Treatments

Two months after the seedlings were transplanted, a completely randomized design (CRD) was conducted to evaluate the effects of the growth status and quality of seedlings in different seasons of July, September, and November. A total of 180 seedlings were tested with 60 seedlings in each tree species, with three replications and 20 seedlings for each replication in each tree species. Except for rainy days, the seedlings were artificially watered daily by natural water consumption to soil saturation. Weeding operations and pest control were carried out on time throughout the experimental period. Photosynthetic physiological measurements were conducted between July–November 2020 after about two months of transplantation.

2.3. Measurement of Gas Exchange Parameters

Per chamber, three plants were randomly selected, and the functional leaves of each plant were marked for measurements. Gas exchange parameters were determined using the LI-6400 portable photosynthesis system (LI-COR, Lincoln, NE, USA). Measurements were made on the upper, mature, and fully expanded leaves from three randomly selected individuals in each treatment. Each individual seedling was measured only once. In the photosynthetic system, CO_2 concentration was 400 µmol mol^{-1} (controlled by a CO_2 cylinder), and irradiances were 1500 $\mu mol \cdot m^{-2} \cdot s^{-1}$. Each measurement was made for 2 min on the upper fully expanded leaves on sunny days between 8:30–11:30 am. The net photosynthetic rate (*Pn*), transpiration rate (*Tr*), stomatal conductance (*Gs*), intercellular CO_2 concentration (*Ci*), and water use efficiency (*WUE*) were obtained by measurement and calculation of gas exchange parameters [26].

2.4. Chlorophyll Fluorescence

Chlorophyll fluorescence was determined using a LI-6400 portable photosynthesis system fitted with a 6400–40 leaf chamber fluorometer. Three to five leaves per treatment were selected for the measurements. Minimal fluorescence (*F0*) of leaves fully exposed to darkness (more than 30 min) was determined after determining the maximum fluorescence (*Fm*). The maximum photochemical quantum yield (*Fv*/*Fm*), non-photochemical quenching coefficient (*NPQ*), photochemical quenching coefficient (*qP*), and photosynthetic electron transport efficiency (*ETR*) were calculated. All measurements were taken at night (7:00–9:00) [27].

2.5. Measurement of Leaf Photosynthetic Pigment

After the photosynthetic measurements, three leaves per treatment were selected to determine the photosynthetic pigments. Leaf chlorophyll (*Chl*) contents were determined following the method of Lichtenthaler [15]. Approximately 0.2 g of fresh leaves was extracted using 25 mL of 95% alcohol grinding, and the absorbance of extracted liquids was recorded at 665 and 649 nm for *Chl* in a spectrophotometer (UU1900, Shanghai Yoke Instrument, China), based on which the contents of *Chl a* and *Chl b* were calculated with formulas [28]:

$$Chl\ a = (11.75\ \mathrm{A662} - 2.35\ \mathrm{A645}) \times \mathrm{V}/\ (1000 \times \mathrm{W})$$

$$Chl\ b = (18.61\ \mathrm{A645} - 3.96\ \mathrm{A662}) \times \mathrm{V}/\ (1000 \times \mathrm{W})$$

$$Chl\ (a + b) = Chl\ a + Chl\ b$$

$$Chl\ a/b = Chl\ a/Chl\ b$$

2.6. Measurement of Leaf Anatomical Characteristics

Tissue dehydration of leaf samples was carried out in alcohol by the following procedure: 70% alcohol for 1/4 h, 85% alcohol for 1/4 h, 90% alcohol for 1/4h, 100% for 1/2 h, and 100% for 1/2 h. Then, leaf samples were embedded in paraffin, cut into 10 µm thick sections, and stained with fast green and safranin. Next, they were mounted, observed, and photographed with an optical microscope (Olympus BX51, Tokyo, Japan) [29]. The resultant digital photos were scaled and analyzed using the ImageJ v1.8.0.112 software (freely available from https://imagej.nih.gov/ij/ (accessed on 25 June 2022)). The measurement of the thickness (µm) of the cross-sectional leaf, palisade parenchyma, and spongy parenchyma, and the difference in thickness of the leaf, upper, and lower epidermal thicknesses was observed on a view of each section at magnifications of 200×. From these measurements, the following parameters were calculated [15]:

$$\text{tightness of leaf tissue} = \text{the length of palisade parenchyma}/\text{leaf thickness} \times 100\%$$

$$\text{tightness of leaf tissue} = \text{the length of spongy parenchyma}/\text{leaf thickness} \times 100\%$$

$$\text{the mesophyll thickness} = \text{palisade tissue thickness} + \text{sponge tissue thickness}$$

$$\text{Palisade sea ratio} = \text{palisade tissue thickness}/\text{Sponge tissue thickness} \times 100\%$$

2.7. Data Analysis

The data were analyzed using a one-way (ANOVA) and mean comparison, and were performed using Duncan's Multiple Range Test at $p < 0.05$ level using SPSS software version 21.0 (SPSS Inc., Chicago, IL, USA), with each treatment consisting of three replicates. The Origin 25.0 software (Origin Laboratory, Northampton, MA, USA) was used to draw the Figures 1–3. The data in the chart is mean ± standard deviation (SD). The effects of physiological and biochemical indices of *Q. chungii*, *Q. gilva,* and *Q. glauca* seedlings were collectively evaluated using the principal component analysis.

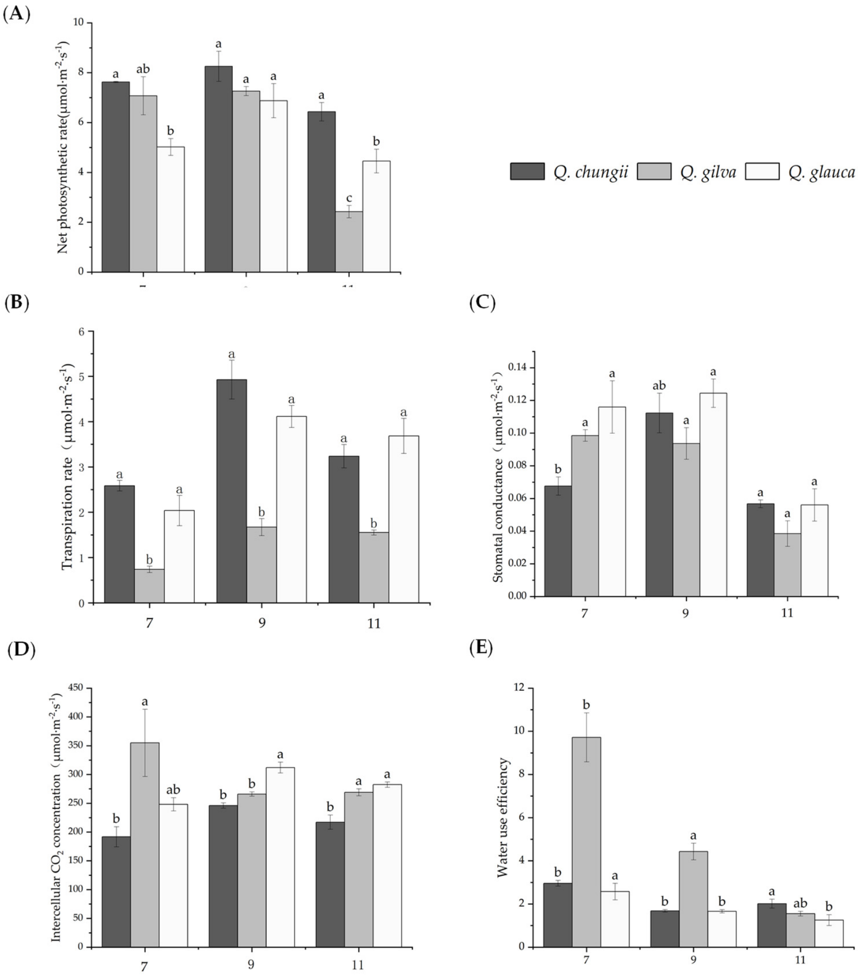

Figure 1. Results of changes in photosynthetic gas exchange parameters in leaves of *Quercus chungii*, *Quercus gilva*, and *Quercus glauca* in the three precious timber species. Data are means ± SD (n = 3). Different lowercase letters following the values indicate significant difference (p < 0.05) between species under the same month. (**A**) net photosynthetic rate (*Pn*), (**B**) stomatal conductance (*Gi*), (**C**) transpiration rate (*Tr*), (**D**) intercellular CO_2 concentration (*Ci*), and (**E**) water use efficiency (*WUE*), 7, 9, and 11 represent July, September, and November, respectively.

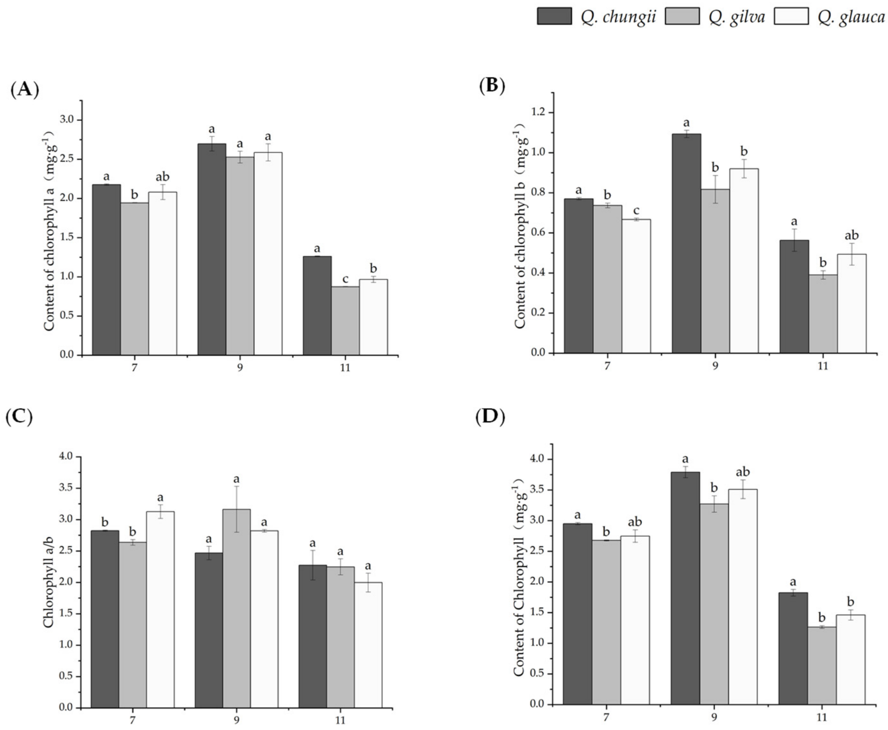

Figure 2. Results of change in photosynthetic pigment on leaves of the three precious timber species of *Q. chungii*, *Q. gilva*, and *Q. glauca*. Data are means ± SD ($n = 3$). Different lowercase letters following the values indicate significant difference ($p < 0.05$) between species under the same month. (**A**) chlorophyll a (*Chl a*), (**B**) chlorophyll b (*Chl b*), (**C**) chlorophyll a/b (*Chl a/b*), and (**D**) contents of chlorophyll (*Chl a + b*).

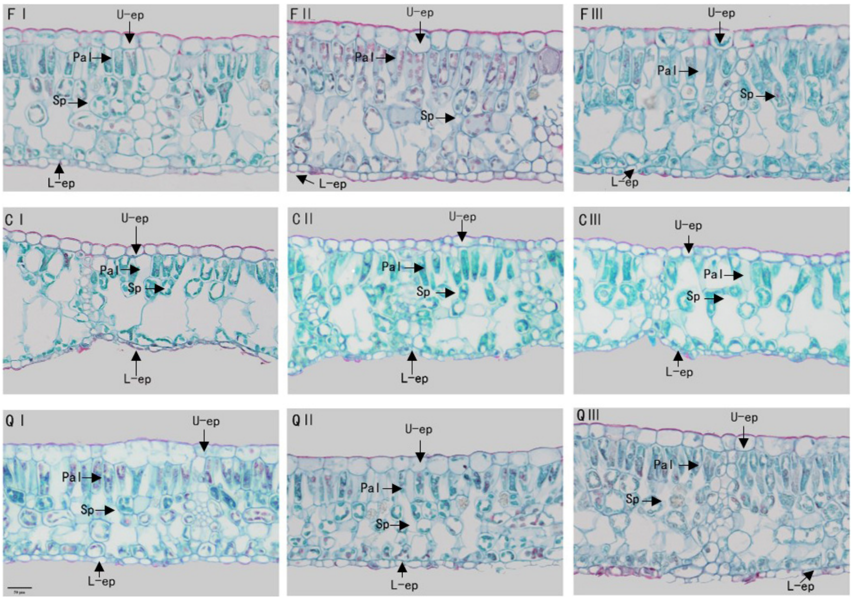

Figure 3. Observation of mature leaf anatomical structure characteristics of *Q. chungii*, *Q. gilva*, and *Q. glauca* seedlings in different months using optical microscopy (×200). U-ep, Upper-epidermis; L-ep: Lower-epidermis; Pal: Palisade; and Sp: Spongy tissue. (F) *Q. chungii*, *Q. gilva*, (Q) *Q. glauca*, (F) *Q. chungii*, (C) *Q. gilva*, (Q) *Q. glauca*, and I, II, III represent July, September, and November respectively.

3. Results

3.1. Changes in Photosynthetic Indexes of Three Precious Timber Species Seedlings of Q. chungii, Q. gilva, and Q. glauca

The results of gas exchange parameters in seedlings of the three *Cyclobalanopsis* species grown under different times showed that photosynthetic characteristics of the three species were significantly different. The maximum results of gas exchange parameters in the seedlings of the three *Cyclobalanopsis* species were observed in September, and the minimum results were observed in November (Figure 1, Table 1). The *Pn*, *Gi*, *Tr*, and *Ci* of the three precious timber species were firstly increased and then decreased during the experimental period. However, the WUE was a downward trend. The *Q. gilva* was significantly higher than *Q. chugii* and *Q. glauca*, and the downward trend was the largest. The order of *Pn* and *Tr* of three tree species in different months was *Q. chugii* > *Q. gilva*> *Q. glauca*. The variation trends of *Gs* and *Ci* were similar: the *Gs* and *Ci* of *Q. chungii* and *Q. glauca* increased first and then decreased. In September, both *Gs* and *Ci* reached the maximum value, but *Q. gilva* showed a downward trend, which reached the minimum value in November (Figure 1). In general, the photosynthetic capacity of the three tree species was in the order: *Q. chungii* > *Q. glauca* > *Q. gilva*.

Table 1. Changes in chlorophyll fluorescence parameters on leaves of the three precious timber species of *Q. chungii*, *Q. gilva*, and *Q. glauca*. (F) *Q. chungii*, Renhua, Guangdong; (C) *Q. gilva*, Jingzhou, Hunan; (Q) *Q. glauca*, Longshan, Hunan; I, II, III represent July, September, and November, respectively. Different letters in the same column indicate significant differences ($p < 0.05$), all data presented are mean ± SD. The same applies below.

Date	Tree Species	*Fo*	*Fm*	*Fv/Fm*	*Y(ΦPSII)*	*ETR*	*qP*	*NPQ*
7	FI	1014.60 ± 31.57 b	4374.04 ± 94.14 a	0.77 ± 0.01 a	0.19 ± 0.02 a	77.71 ± 9.09 a	0.31 ± 0.03 a	2.61 ± 0.12 a
	CI	1133.90 ± 33.03 a	4548.44 ± 217.92 a	0.75 ± 0.01 b	0.12 ± 0.01 b	44.40 ± 4.03 b	0.15 ± 0.02 b	1.82 ± 0.09 c
	QI	1022.03 ± 16.78 b	4481.36 ± 22.17 a	0.76 ± 0.01 a	0.12 ± 0.01 b	46.04 ± 3.08 b	0.16 ± 0.01 b	2.22 ± 0.06 b
9	FII	1103.49 ± 16.61 b	4667.43 ± 38.69 b	0.76 ± 0.01 a	0.17 ± 0.02 a	64.44 ± 8.29 a	0.24 ± 0.04 a	2.49 ± 0.12 a
	CII	1222.62 ± 25.77 a	5006.25 ± 122.61 a	0.76 ± 0.01 a	0.16 ± 0.02 a	64.90 ± 6.55 a	0.25 ± 0.03 a	2.60 ± 0.15 a
	QII	1095.10 ± 19.00 b	4534.65 ± 97.82 b	0.76 ± 0.01 a	0.12 ± 0.01 a	44.24 ± 3.41 a	0.15 ± 0.02 a	2.02 ± 0.37 b
11	FIII	1149.65 ± 48.00 a	3678.01 ± 152.21 a	0.68 ± 0.02 b	0.12 ± 0.01 a	56.07 ± 9.08 a	0.19 ± 0.05 a	1.73 ± 0.019 a
	CIII	1215.85 ± 72.39 a	3691.49 ± 136.57 a	0.76 ± 0.01 a	0.12 ± 0.01 a	48.97 ± 5.24 a	0.20 ± 0.03 a	1.68 ± 0.08 b
	QIII	1166.86 ± 40.77 a	3165.23 ± 138.84 b	0.63 ± 0.03 b	0.12 ± 0.01 a	48.71 ± 5.11 a	0.19 ± 0.02 a	1.21 ± 0.10 a

3.2. Changes in Chlorophyll Fluorescence Parameters of Three Precious Timber Species seedlings of Q. chungii, Q. gilva, and Q. glauca

There were also significant differences in chlorophyll fluorescence parameters between the three species (Table 1). However, the changes in *Fo* and *Fm* in different months were non-significant. The *Fo* values of *Q. chungii*, *Q. gilva*, and *Q. glauca* increased significantly with time since July and increased by 8.76%, 7.82%, and 6.81%, respectively, in September. The *Fm* value increased first and then decreased, peaking in September, and the electron transfer capacity is the largest. In the PSII reaction center, the *Y (II)* of *Q. chungii* in July was significantly higher than that of *Q. glauca* and *Q. gilva* by 36.84%, 5.88%, and 29.41%, respectively, in September. At the same time, the *ETR*, *qP*, and *NPQ* values of *Q. chungii* were also about 50% higher than those of *Q. glauca* and *Q. gilva*. The results showed that the electron transfer efficiency of *Q. chungii* was the highest, and the electron transfer of the PSII reaction center was the most active (Table 1).

3.3. Changes in Photosynthetic Pigments in Seedlings of Three Precious Timber Species of Q. glauca, Q. gilva and Q. chungii

The results showed that the contents of *Chl a*, *Ch b*, *Chl a/b*, and chloroplast pigment were significantly different among the three tree species ($p < 0.05$, Figure 2). All three tree species exhibited a higher *Chl a*, *Chl b*, and *Ch a/b* when plants were subjected to sunlight during September (Figure 2). Except for July, the *Chl a*, *Chl b*, and *Chl* total values of *Q. chungii* were significantly higher than those of *Q. gilva* and *Q. glauca* in the other two periods. Even in November, the *Chl* total of *Q. glauca* was still 193% and 170% higher than that of *Q. gilva* and *Q. glauca*, respectively. The *Chl* total of *Q. chungii* was significantly higher than that of *Q. gilva* and *Q. glauca*, which indicated that *Q. chungii* had a stronger light energy capture ability.

3.4. Analysis on Leaf Anatomical Structure of Three Precious Timber Species of Q. chungii, Q. gilva, and Q. glauca

There were also significant differences in leaf anatomical traits between the three species (Figure 3, Table 2). The leaf anatomical structures of plants were composed of epidermis, palisade tissue, spongy tissue, and leaf veins. The leaf epidermis includes the upper epidermis and the lower epidermis. The upper and lower epidermis were composed of one layer of closely arranged cells, and the upper epidermal cells were significantly larger than the lower epidermal cells. It was found that the upper epidermal cells of *Q. chungii* and *Q. glauca* were elliptical and nearly square, and the leaf thickness of *Q. chungii* seedlings was the thickest 89.91 ± 8.19 µm, followed by *Q. glauca* 259.75 ± 5.58 µm. However, the upper epidermal cells of *Q. gilva* were flat and nearly rectangular and had the thinnest leaves 218.32 ± 4.19 µm (Table 2). From July to September, leaf thickness and upper and lower epidermis thickness increased significantly. The changing trend of palisade and spongy tissue volume of *Q. chungii* and *Q. glauca* was smaller from July to September, while that of *Q. gilva* was thicker (Table 2). Although the tissue tightness and looseness of leaves of each tree species did not show obvious regular changes in different growth periods, the transitions between different months were also significant. The tightness of *Q. glauca* decreased by 3% and the porosity gradually increased by 4% (Table 2). In September, the palisade tissue and sponge tissue of *Q. chungii* reached the minimum (Figure 3FII), and the tightness and porosity reached their minimum values of 0.25 and 0.54, respectively (Table 2). Whereas, in November, the compactness of *Q. gilva* tightness and porosity both reached a minimum value of 0.27 and 0.55 (Figure 3QIII, Table 2).

Table 2. Leaf structural traits of the three precious timber species of *Q. chungii*, *Q. gilva*, and *Q. glauca*. Data are means ± SD (n = 5). Different lowercase letters following the values indicate significant differences ($p < 0.05$) between species under the same month.

Date		Leaf	Palisade Tissue	Spongy Tissue	Lower Epidermis	Upper Epidermis	Ratio of Palisade Tissue and Spongy Tissue	Cell Tense Ratio	Spongy Tissue Looseness
Month		Thickness (µm)							
7	FI	253.13 ± 7.15 a	63.17 ± 2.10 a	145.49 ± 3.16 a	14.44 ± 0.88 a	30.04 ± 1.13 a	0.43 ± 0.01 b	0.25 ± 0.01 b	0.58 ± 0.01 a
	CI	190.36 ± 6.30 c	54.13 ± 2.01 b	105.95 ± 4.33 c	11.17 ± 0.74 b	19.12 ± 0.50 b	0.51 ± 0.02 a	0.28 ± 0.01 a	0.56 ± 0.01 a
	QI	225.50 ± 6.18 b	63.17 ± 2.10 a	120.56 ± 2.12 b	12.46 ± 0.67 ab	29.32 ± 1.38 a	0.52 ± 0.01 a	0.28 ± 0.01 a	0.53 ± 0.02 b
9	FII	244.30 ± 6.11 a	61.06 ± 1.75 a	130.85 ± 2.34 a	15.32 ± 0.88 a	37.08 ± 1.25 a	0.47 ± 0.01 b	0.25 ± 0.02 c	0.54 ± 0.01 b
	CII	218.32 ± 4.19 b	61.48 ± 1.22 a	122.03 ± 1.51 b	11.04 ± 0.55 b	23.77 ± 0.98 c	0.50 ± 0.01 a	0.28 ± 0.01 a	0.56 ± 0.01 a
	QII	221.35 ± 7.34 b	58.16 ± 2.34 a	116.22 ± 3.68 b	16.03 ± 0.43 a	30.95 ± 1.22 b	0.50 ± 0.01 a	0.27 ± 0.01 b	0.53 ± 0.02 b
11	FIII	289.91 ± 8.19 a	74.20 ± 0.82 a	163.62 ± 5.88 a	14.75 ± 0.66 b	37.34 ± 1.18 a	0.46 ± 0.01 b	0.26 ± 0.01 b	0.57 ± 0.01 a
	CIII	198.57 ± 6.67 c	53.74 ± 2.54 c	109.82 ± 3.54 c	12.27 ± 0.35 c	22.74 ± 0.57 c	0.49 ± 0.01 a	0.27 ± 0.01 a	0.55 ± 0.01 b
	QIII	259.75 ± 5.58 b	63.97 ± 1.80 b	147.77 ± 2.85 b	16.95 ± 0.34 a	31.06 ± 0.67 b	0.43 ± 0.01 c	0.25 ± 0.01 b	0.57 ± 0.01 a

3.5. Principal Component Analysis (PCA)

PCA analysis was illustrated using a bi-dimensional plot in which components PC1 and PC2 explain 68.7%, 69.9%, and 79.2% of data variability of changes in photosynthetic indexes, chlorophyll fluorescence parameters, photosynthetic pigments, and leaf anatomical structure pigments in July, September, and November (Figure 4). Results indicated that *Q. chungi* had a high positive correlation with changes in photosynthetic indexes, chlorophyll fluorescence parameters, photosynthetic pigments, and leaf anatomical structure pigments in September (Figure 4A), while *Q. gilva* did not correlate with leaf anatomical structure pigments (Figure 4B). Similarly, there was a high positive correlation with changes in photosynthetic indexes, chlorophyll fluorescence parameters and photosynthetic pigments in the *Q. glauca* (Figure 4C).

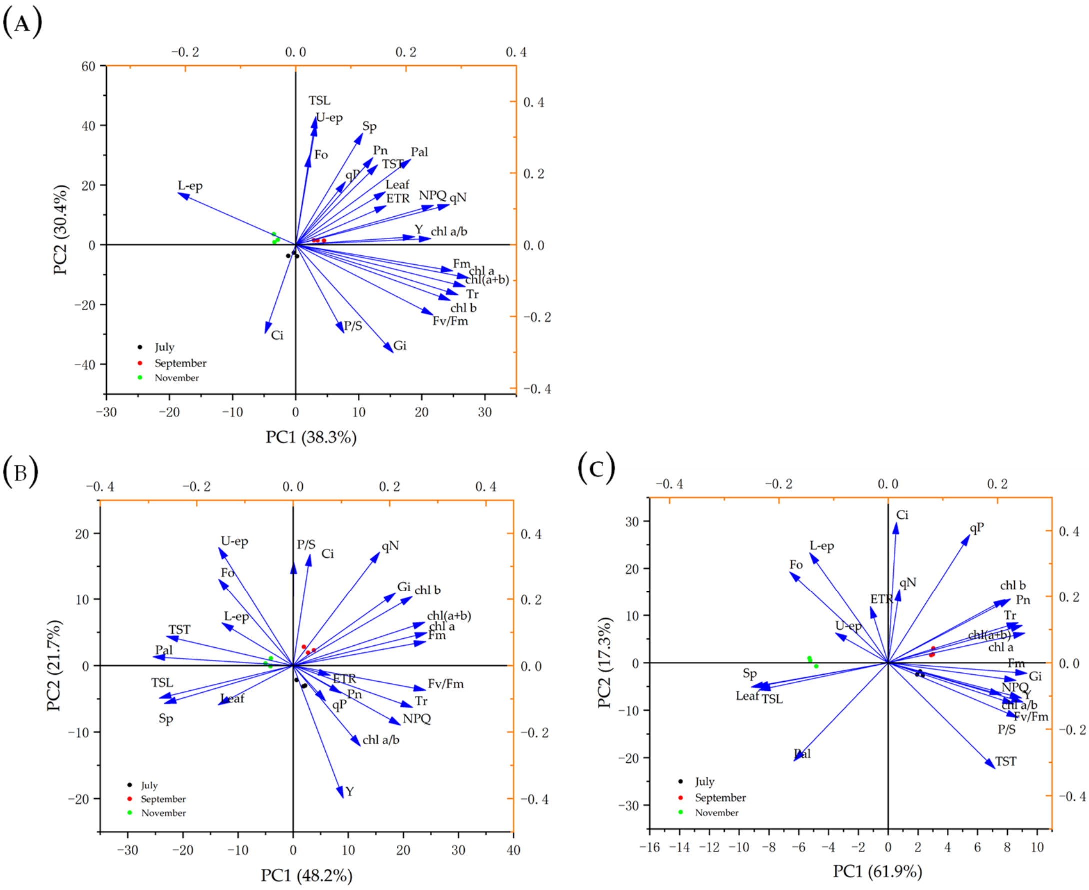

Figure 4. Principal component analysis (PCA) describing the responses of *Q. chungi* (**A**), *Q. gilva* (**B**), and *Q. glauca* (**C**) of photosynthetic characteristics and leaf anatomical structure parameters in July, September, and November. (*Pn*) net photosynthetic rate ($\mu mol \cdot m^{-2} \cdot s^{-1}$), (*Tr*) transpiration rate ($\mu mol \cdot m^{-2} \cdot s^{-1}$), (*Gi*) stomatal conductance ($\mu mol \cdot m^{-2} \cdot s^{-1}$), (*Ci*) intercellular CO_2 concentration ($\mu mol \cdot m^{-2} \cdot s^{-1}$), (*U-ep*) upper-epidermis (μm), (*Pal*) palisade (μm), (*Sp*) spongy tissue (μm), (L-ep) lower-epidermis, (*P/S*) ratio of palisade tissue and spongy tissue, (leaf) leaf thickness (μm), (*TST*) cell tense ratio, (*TSL*) spongy tissue looseness, (*Chl* (*a* + *b*)) the total of Chlorophyll ($mg \cdot g^{-1}$), (*Chl a*) Chlorophyll a ($mg \cdot g^{-1}$), (*Chl b*) Chlorophyll b ($mg \cdot g^{-1}$), (*Chl a/b*) Chlorophyll a/b, and Chlorophyll fluorescence parameters (*Fo*, *Fv*/*Fm*, *ETR*, *qP*, *Y*, and *NPQ*).

4. Discussion

Our results showed that the three *Cyclobalanopsis* species diverged significantly in photosynthetic characteristics and pigment. In this study, the one-year-old seedlings of *Q. chungii*, *Q. gilva*, and *Q. glauca* were used to evaluate their growth and ecological adaptation potential in response to natural high-temperature environmental stress for afforestation. The seasonal differences were observed among three tress species seedlings by the measurement on photosynthetic parameters of gas exchange, chlorophyll fluorescence parameters, photosynthetic pigment content, and paraffin section observation of leaf anatomical structure of seedlings in July, September, and November. Seedlings of the three congeneric tree species adapted to the same environments but diverged substantially in characteristics related to resistant tolerance. Those findings facilitate the understandings of cultivation on the three different *Quercus* L. section *Cyclobalanopsis* seedlings of *Q. chungii*, *Q. gilva*, and *Q. glauca* and provide basic research data for the selection of precious timber afforestation tree species in subtropical areas.

4.1. Differences in Photosynthetic Gas Exchange among the Three Species

The gas exchange parameters *Pn*, *Gs*, *Tr*, *Ci*, and *WUE* were significantly different among the three precious timber species. Some studies had shown that Korean pines (*Pinus koraiensis*) had higher *Gs* in September, but the high photosynthetic rate of tree species was at the cost of a high transpiration rate, which required a large amount of intercellular CO_2 and water supply [30]. Plants can reduce leaf surface temperature by increasing transpiration rate, so that leaves can be protected from damage in a high-temperature environment, thereby maintaining a high photosynthetic rate [31]. In this study, the *Pn* and *Tr* values of *Q. chungii* increased significantly and peaked in September, which was higher than that of *Q. gilva* and *Q. glauca*. In addition, combined with Figure 1 and Table 2, it was found that the leaf structure of *Q. gilva* did not change significantly under high temperatures through efficient water use efficiency in the natural environment. Moreover, the high-temperature intrinsic water use efficiency was significantly higher during July and September than in November of *Q. chungii* and *Q. glauca* [32]. Therefore, compared with *Q. gilva* and *Q. glauca*, *Q. chungii* can maintain a higher photosynthetic capacity under a natural drought-stress environment and has a strong ecological adaptability adjustment ability [33].

4.2. Differences in Chlorophyll Fluorescence Parameters among the Three Species

Chl fluorescence was affected by light intensity and water deficit stress in different plant growth stages. Therefore, the *F0*, *Fm*, *Fv*, *Fv*/*Fm*, *NPQ*, *qP*, and *Y* values are the most important Chl fluorescence parameters which are broadly used in plant stress physiology studies [34]. An increase in F0 represents any difficulty and degradation in photosystem II, or any disruption in energy transfer into the reaction center. It has been reported that F0 would increase under full-stress conditions, but the *Fv*/*Fm* ratio would be reduced [25,35]. In this study, *F0* significantly increased due to natural drought induced by high temperatures. Other researchers have found similar results [36]. The *qP* value approximates the proportion of PSII reaction centers that are open. In other words, *qP* represents the energy consumed in photosynthesis. On the other hand, *NPQ* is the amount of dissipated excessive irradiation into heat. *NPQ* represents an effective way as to how photosynthetic organisms can dissipate excessive irradiation into heat [37]. Studies on *NPQ* can help to understand the xanthophyll cycle activity [38]. The ΦPSII value gives an estimation of the efficiency and represents the photochemistry at different photon flux densities [39]. In this study, the *Y* of *Q. chungii* was significantly higher than in *Q. gilva* and *Q. glauca*. The *Q. chungii* showed the highest ability to acclimate to mild heat stress during the vegetation season to prevent heat-related damage at the Y level. In addition, the *qP* and *ETR* values of *Q. chungii* were also higher than those of *Q. gilva* and *Q. glauca*.. The greater the *qP* value, the greater the opening degree of the PSII reaction center, and the highest PSII electron transport activity, which indicated that the opening degree of the PSII reaction center and the electron transport activity of PSII in photosynthesis of *Q. chungii* were higher than those of the other two species. It was therefore observed that *Q. chungii* had the potential to improve the potential photochemical activity more than the other two tree species, and the high content of photosynthetic pigments could also accelerate the electron transfer rate and promote the actual photosynthetic capacity.

4.3. Difference in Photosynthetic Pigments in Leaves among the Three Species

There was strong coordination between leaf photosynthetic pigment and photosynthetic gas exchange. During the same month, the net photosynthetic rate of *Q. chungii* was the highest among tree species. In the test period, the contents of *Chl a*, *Chl b*, and *Chl* total increased first and then decreased, and reached the peak in September, which was consistent with the changing trend of photosynthetic rate *Pn* of the three species. It shows that the three precious timber species had the highest efficiency of light energy absorption and utilization in September. Those findings were identical to the results of the study on Chlorophyll content of Terminthia paniculata [40]. The measured *Chl a* and *Chl b* values of *Q. chungii* were significantly higher than those of *Q. gilva* and *Q. glauca*, indicating that *Q. chungii* had a stronger ability to absorb and transfer light energy. The *Chl a/b* value can also be used as one of the indexes to evaluate plant stress resistance [41]. The *Chl a* and *Chl b* contents of *Q. chungii* were significantly higher than those of *Q. gilva* and *Q. glauca*, which was related to the species specificity in the photosynthesis regulation mechanism of different tree species in response to habitat stress [42].

4.4. Difference in Leaf Anatomical Structure of Three Plants and Their Response to Natural Drought

Just as how the significant differences in photosynthetic characteristics are observed, the three species also diverge substantially in leaf anatomical-related traits. *Q. chungii* has obvious xerophytic structural characteristics, such as thicker leaves, a smaller ratio of palisade tissue, and spongy tissue, which is consistent with the plants adapted to the dry and hot habitats in their natural distributions [43]. The anatomical structure of the leaves of the three *Cyclobalanopsis* species varied significantly with time showing a relatively high degree of plasticity to adapt to natural drought conditions. The experimental results were similar to European beech (*Fagus sylvatica* L.), and all tree species showed robust physiological and morphological adaptation, in combination with growth and anatomy [44]. The thickness of leaf and palisade tissue was reduced, tissue structure tightness was enhanced, and the porosity was reduced with time, which was conducive to more effective adaptation to drought stress induced by high temperature [22]. This was consistent with the results of the study in various plant trees, i.e., *olive* (*Olea europaea*) and tea (*Camellia oleifera*) leaves under different drought stress [45,46]. The tolerance to drought stress of *Q. chungii* seedlings was further confirmed by the observations of *Q. chungii* leaves under high temperature conditional, while the *Q. gilva* and *Q. glauca* had no significant structural changes. Populations of *Q. chungii* with drought adapted traits would represent highly desirable plant material for afforestation under climate change.

5. Conclusions

A seasonal variation in photosynthetic and leaf anatomical structure in seedlings of the three *Cyclobalanopsis* species was measured simultaneously for the first time. The differences in photosynthetic and leaf anatomical structure in seedlings of the three *Cyclobalanopsis* species reflect large differences in their growth environment under natural conditions. These findings contribute to a deeper understanding of the physiological ecology related to the natural adaptability of the three tree species for afforestation. Fundamental *Q. chungii* was more adaptable to high-temperature conditions compared to the other two species, which is an excellent significance for successful application in the installation of afforestation. The strong drought resistance and photosynthetic efficiency of *Q. chungii* seedlings indicate that this endangered species is more suitable for subtropical regions where seasonal drought often occurs in summer. More exploration on the characteristics of precious tree species for high-valuable timber resource development should be addressed in the future.

Author Contributions: Conceptualization, M.-H.Y.; Data curation, H.-M.Y., P.-L.L. and W.-H.D.; Formal analysis, H.-M.Y. and H.X.; Funding acquisition, M.-H.Y.; Investigation, H.-M.Y., P.-L.L., Q.-Y.X., F.-L.Z., Y.C. and Y.J.; Project administration, M.-H.Y. and X.-L.Y.; Resources, X.-L.Y.; Supervision, M.-H.Y.; Writing—original draft, H.-M.Y. and M.-H.Y.; and Writing—review & editing, H.-M.Y., M.-H.Y. and Y.-L.L. All authors have read and agreed to the published version of the manuscript.

Funding: This research was supported by Special Fund for Innovative Province Construction in Hunan (Grant No. 2020NK2017).

Data Availability Statement: The samples analyzed may be available upon request after a share transfer agreement. The datasets generated during the current study are available from the corresponding author upon reasonable request.

Acknowledgments: The authors thank Wen-Fei Zhang for his help and support in producing plants. And thank Feng Zou and Ze Li in the Key Laboratory of Cultivation and Protection for Non-Wood Forest Trees, Central South University of Forestry and Technology, for their support in the experimental apparatus.

Conflicts of Interest: The authors declare no conflict of interest.

References

1. Nixon, K.C. Global and neotropical distribution and diversity of oak (genus *Quercus*) and oak forests. In *Ecology and Conservation of Neotropical Montane Oak Forests (Ecological Studies)*; Springer: Berlin/Heidelberg, Germany, 2006; pp. 3–13.
2. Huang, C.C.; Chang, Y.T.; Bartholomew, B. Fagaceae. In *Flora of China*; Wu, C.Y., Raven, P.H., Eds.; Science Press: Beijing, China, 1999; Volume 4, pp. 314–400.
3. Denk, T.; Grimm, G.W.; Manos, P.S.; Deng, M.; Hipp, A.L. An updated infrageneric classification of the oaks: Review of previous taxonomic schemes and synthesis of evolutionary patterns. In *Oaks Physiological Ecology. Exploring the Functional Diversity of the Genus Quercus L.*; Gil-Pelegrin, E., Peguero-Pina, J.J., Sancho-Knapik, D., Eds.; Springer: Berlin/Heidelberg, Germany, 2017; pp. 13–38.
4. Gil-Pelegrin, E.; Peguero-Pina, J.J.; Sancho-Knapik, D. (Eds.) Oaks and people: A long journey together. In *Oaks physiological Ecology. Exploring the functional diversity of the genus Quercus L.*; Springer: Berlin/Heidelberg, Germany, 2017; pp. 1–12.
5. Li, Z.H.; Li, B.H.; Qi, C.J.; Yu, X.L.; Wu, Y. Studies on importance of valuable wood species resources and its development strategy. *J. Cent. South Univ. For. Technol.* **2013**, *32*, 1–8.
6. Carrero, C.; Jerome, D.; Beckman, E.; Byrne, A.; Coombes, A.J.; Deng, M.; González-Rodríguez, A.; Van Sam, H.; Khoo, E.; Nguyen, N.; et al. *The Red List of Oaks 2020*; The Morton Arboretum: Lisle, IL, USA, 2020; pp. 30–44.
7. Wang, Y.; Wu, P.; Wang, R.; Ma, X.; Zhou, X. Community characteristics of *Cyclobalanopsis chungii* forest in Mingqing nature reserve. *J. Fujian Agric. For. Univ.* **2011**, *40*, 37–42.
8. Liu, A.-Q.; Liu, C.-H.; Ma, X.-Q. Study on biomass production of *Cyclobalanopsis chungii* plantation. *J. Fujian College For.* **2004**, *24*, 294–297.
9. Liu, N.; Li, Z.; Wang, P.; Li, H. Biomass estimation of the growth law of *Cyclobalanopsis gilva* plantations. *J. Cent. South Univ. For. Technol.* **2022**, *42*, 143–149.
10. Xia, C.; Li, H.; Wang, P.; Li, Z.; Wang, B.; Zhu, Z. Effects of shading on the photosynthetic characteristics of *Cyclobalanopsis gilva* seedlings. *J. Cent. South Univ. For. Technol.* **2021**, *41*, 72–79.
11. Zhang, B.; Zhu, N.; Cao, J. Effects of habitats on photosynthesis characteristics of *Cyclobalanopsis gilva*. *J. South China Agric. Univ.* **2017**, *38*, 70–78.
12. Xie, J. Interspecific relationships and ecological species division of dominant populations of natural forest in *Cyclobalanopsis gilva*. *J. Sichuan Agric.Univ.* **2020**, *38*, 127–134.
13. Gu, D.; Zhang, Z.; Mallik, A.; Zhou, A.; Mo, L.; He, C.; Huang, Y. Seasonal water use strategy of *Cyclobalanopsis glauca* in a karst area of southern China. *Environ. Earth. Sci.* **2015**, *74*, 1007–1014. [CrossRef]
14. Gratani, L. Plant phenotypic plasticity in response to environmental factors. *Adv. Bot.* **2014**, 1–17. [CrossRef]
15. Wu, Y.; Hong, W.; Chen, Y. Leaf physiological and anatomical characteristics of two indicator species in the limestone region of Southern China under drought Stress. *Pak. J. Bot.* **2018**, *50*, 1335–1342.
16. Brodribb, T.J.; Powers, J.; Cochard, H.; Choat, B. Hanging by a thread? Forests and drought. *Science* **2020**, *368*, 261–266. [CrossRef] [PubMed]
17. Iszkulo, G. Success and failure of endangered tree species: Low temperature and low light availability affects survival and growth of European yew (*Taxus baccata* L.) Seedlings. *Pol. J. Ecol.* **2010**, *58*, 259–271.
18. Adams, W.W.; Stewart, J.J.; Demmig-Adams, B. Photosynthetic modulation in response to plant activity and environment. In *The Leaf: A Platform for Performing Photosynthesis*; Adams, W.W., Terashima, I., Eds.; Springer: Berlin/Heidelberg, Germany, 2018; pp. 493–563.
19. Momayyezi, M.; Borsuk, A.M.; Brodersen, C.R.; Gilbert, M.E.; Théroux-Rancourt, G.; Kluepfel, D.A. Desiccation of the leaf mesophyll and its implications for CO_2 diffusion and light processing. *Plant Cell Environ.* **2022**, *45*, 1362–1381. [CrossRef] [PubMed]
20. Maxwell, K.; Johnson, G.N. Chlorophyll fluorescence—A practical guide. *J. Exp. Bot.* **2000**, *51*, 659–668. [CrossRef]
21. Wei, L.; Huang, Y.; Li, X.; Mo, L.; Yuan, W. Effects of soil water on photosynthetic characteristics and leaf traits of *Cyclobalanopsis glauca* seedlings growing under nutrient-rich and-poor soil. *Acta Ecol. Sin.* **2009**, *29*, 160–165. [CrossRef]
22. Wu, L.; Li, Z.; Yang, M.; Wang, P. Response of leaf anatomical characteristics of *Cyclobalanopsis gilva* seedlings to drought stress. *J. Appl. Ecol.* **2015**, *26*, 3619–3626.
23. Xue, L.; Ren, H.; Long, W.; Leng, X.; Wang, J.; Yao, X.; Li, S. Ecophysiological responses of calcicole *Cyclobalanopsis glauca* (Thunb.) oerst. to drought stress and calcium supply. *Forests* **2018**, *9*, 667. [CrossRef]
24. Sai, W.; Li-Ta, Y.; Shu-Quan, Y.; Chao, Z.; Jing-Jing, S. Effects of simulating acid rain on photosynthesis and chlorophyll fluorescence parameters of *Quercus glauca*. *J. Appl. Ecol.* **2014**, *25*, 2183–2192.

25. Wang, A.-Y.; Hao, G.-Y.; Guo, J.-J.; Liu, Z.-H.; Zhang, J.-L.; Cao, K.-F. Differentiation in leaf physiological traits related to shade and drought tolerance underlies contrasting adaptations of two *Cyclobalanopsis* (Fagaceae) species at the seedling stage. *Forests.* **2020**, *11*, 844. [CrossRef]
26. Bassman, J.H.; Zwier, J.C. Gas exchange characteristics of *Populus trichocarpa*, *Populus deltoides* and *Populus trichocarpa* × *P. deltoides* clones. *Tree Physiol.* **1991**, *8*, 145–159. [CrossRef]
27. Hao, J.-Q.; Zhang, L.; Zheng, C.-X.; Bai, X.; Li, W.-H. Differences in chlorophyll fluorescence parameters and water content in heteromorphic leaves of *Populus euphratica* from Inner Mongolia, China. *For. Stud. China.* **2011**, *13*, 52–56. [CrossRef]
28. Lightenthaler, H. Chlorophylls and carotenoids: Pigments of photosynthetic biomembranes. *Meth. Enzymol.* **1987**, *148*, 350–382.
29. Liu, Q.; Li, Z.; Wu, J. Research progress on leaf anatomical structures of plants under drought stress. *J. Agric. Sci. Technol.* **2016**, *17*, 4–7.
30. Makoto, K.; Koike, T. Effects of nitrogen supply on photosynthetic and anatomical changes in current-year needles of *Pinus koraiensis* seedlings grown under two irradiances. *Photosynthetica* **2007**, *45*, 99–104. [CrossRef]
31. Oguchi, R.; Onoda, Y.; Terashima, I.; Tholen, D. Leaf Anatomy and Function. In *The Leaf: A Platform for Performing Photosynthesis*; Advances in Photosynthesis and Respiration; Adams, W., III, Terashima, I., Eds.; Springer: Berlin/Heidelberg, Germany, 2018; Volume 44, pp. 97–139.
32. Petrik, P.; Petek-Petrik, A.; Konôpková, A.; Fleischer, P.; Stojnic, S.; Zavadilova, I.; Kurjak, D. Seasonality of PSII thermostability and water use efficiency of in situ mountainous Norway spruce (*Picea abies*). *J. For. Res.* **2022**, *32*, 1–12. [CrossRef]
33. Ashraf, M. Relationships between leaf gas exchange characteristics and growth of differently adapted populations of Blue panicgrass (*Panicum antidotale* Retz.) under salinity or waterlogging. *Plant Sci.* **2003**, *165*, 69–75. [CrossRef]
34. Zheng, C.; Qiu, J.; Jiang, C.; Yue, N.; Wang, X.; Wang, W. Comparison of stomatal characteristics and photosynthesis of polymorphic *Populus euphratica* leaves. *Front Agric China.* **2007**, *2*, 87–93. [CrossRef]
35. Misra, A.N.; Misra, M.; Singh, R. Chlorophyll fluorescence in plant biology. *Biophysics* **2012**, *7*, 171–192.
36. Björkman, O.; Demmig, B. Photon yield of O_2 evolution and chlorophyll fluorescence characteristics at 77 K among vascular plants of diverse origins. *Planta* **1987**, *170*, 489–504. [CrossRef]
37. Li, G.; Wu, H.; Sun, Y.; Zhang, S. Response of chlorophyll fluorescence parameters to drought stress in sugar beet seedlings. *Russ. J. Plant Physiol.* **2013**, *60*, 337–342. [CrossRef]
38. Hampton, J.G.; TeKrony, D.M. *Handbook of Vigour Test Methods*; The International Seed Testing Association: Zurich, Switzerland, 1995.
39. Cabrera-Bosquet, L.; Albrizio, R.; Araus, J.L.; Nogués, S. Photosynthetic capacity of field-grown durum wheat under different N availabilities: A comparative study from leaf to canopy. *Environ. Exp. Bot.* **2009**, *67*, 145–152. [CrossRef]
40. Húdoková, H.; Petrik, P.; Petek-Petrik, A.; Konôpková, A.; Leštianska, A.; Střelcová, K.; Kmeť, J.; Kurjak, D. Heat-stress response of photosystem II in five ecologically important tree species of European temperate forests. *Biologia* **2022**, *77*, 671–680. [CrossRef]
41. Gitelson, A.; Merzlyak, M.N. Quantitative estimation of chlorophyll-a using reflectance spectra: Experiments with autumn chestnut and maple leaves. *J. Photochem. Photobiol. B Biol.* **1994**, *22*, 247–252. [CrossRef]
42. Liying, X.; Yuping, H.; Gang, W. Effect of water stress on pigment content and PAL activity of purple leaf plum. *J. Jilin Univ. Inf. Sci. Ed.* **2007**, *29*, 168–172.
43. Wright, I.J.; Reich, P.B.; Westoby, M.; Ackerly, D.D.; Baruch, Z.; Bongers, F.; Cavender-Bares, J.; Chapin, T.; Cornelissen, J.H.; Diemer, M. The worldwide leaf economics spectrum. *Nature* **2004**, *428*, 821–827. [CrossRef] [PubMed]
44. Petrik, P.; Petek-Petrik, A.; Kurjak, D.; Mukarram, M.; Klein, T.; Gömöry, D.; Střelcová, K.; Frýdl, J.; Konôpková, A. Interannual adjustments in stomatal and leaf morphological traits of European beech (*Fagus sylvatica* L.) demonstrate its climate change acclimation potential. *Plant Biol.* **2022**, *24*, 1287–1296. [CrossRef]
45. Ennajeh, M.; Vadel, A.; Cochard, H.; Khemira, H. Comparative impacts of water stress on the leaf anatomy of a drought-resistant and a drought-sensitive olive cultivar. *J. Hortic. Sci. Biotechnol.* **2010**, *85*, 289–294. [CrossRef]
46. Hu, Y.; Yang, L.; Gao, C.; Liao, D.; Long, L.; Qiu, J.; Wei, H.; Deng, Q.; Zhou, Y. A comparative study on the leaf anatomical structure of *Camellia oleifera* in a low-hot valley area in Guizhou Province, China. *PLoS ONE* **2022**, *17*, e0262509. [CrossRef]